Role of higher order couplings in the presence of kaons in relativistic mean field description of neutron stars

Neha Gupta* and P. Arumugam

Department of Physics, Indian Institute of Technology Roorkee, Roorkee - 247 667, India

(Dated: March 2, 2013)

We discuss the role of higher order couplings in conjunction with kaon condensation using recent versions of relativistic mean field models. We focus on an interaction (G2) in which all parameters are obtained by fitting finite nuclear data and successfully applied to reproduce variety of nuclear properties. Our results show that the higher order couplings play a significant role at higher densities where kaons dominate the behavior of equation of state. We compare our results with other interactions (NLl, NL3, G1 and FSUGold) and show that the new couplings bring down the mass of neutron star (NS), which is further reduced in the presence of kaons to yield results consistent with present observational constraints. We show that the composition of NS vary with the parameter sets.

I. INTRODUCTION

Neutron stars (NS) provide us with opportunities to probe the properties of matter at extremely high densities, and have proven to be fantastic test bodies for theories involving general relativity. In a broader perspective NS provide access to the phase diagram of matter at extreme densities and temperatures, which is the basic for understanding very early Universe and several other astro-physical phenomena. The observational quantities of primary astrophysical interest are the maximum mass and the typical radius of a NS. Neuron stars are detected as pulsar+NS or pulsar+white-dwarf or X-ray binaries. Recent observations of pulsars and X-ray binaries suggest that the maximum mass of a NS lies between $1-2\ M_\odot$ [1–6], where $M_\odot$ is the solar mass.

To understand the observables of NS, various theoretical models have been developed and can be grouped into three broad categories [7]: nonrelativistic potential models [8–10], relativistic field theoretical models [11] and Dirac-Brueckner-Hartree-Fock models [12, 13]. In each of these models, the addition of hyperon [14] or kaon or pion [15–18] or quarks [16] or their combinations, will soften the equation of state (EoS) and hence lower the maximum mass of NS. In all of these models, coupling constants and unknown meson masses are treated as effective parameters adjusted to fit the empirical quantities (saturation density ρ_0, binding energy E/A, compression modulus K_∞, effective nucleon mass m_n^* and asymmetry energy J) at nuclear saturation. The compression modulus (K_∞) defines the curvature of the EoS at saturation density and its value will be reflected in the high density behaviour (stiffness or softness) of the EoS. Thus K_∞ will have a direct bearing on the maximum mass. Interestingly, the study of isoscalar giant resonances can reveal rich information about nuclear compressibility [19, 20].

The EoS and hence the NS radius can directly be linked to the neutron skin thickness in heavy nuclei [21–23]. These strong links between the NS structure and finite nuclear properties prove that the knowledge in these two areas complement each other.

One among the very-well tested model in finite nuclei is the nonlinear $\sigma-\omega-\rho$ model, widely mentioned as relativistic mean field (RMF) model [24]. The RMF model constructed with idea of renormalizability, produces accurate results for spherical and deformed nuclei but it gives a very stiff EoS for infinite nuclear matter. Recently, inspired by effective field theory (EFT) Furnstahl, Serot and Tang [25] abandoned the idea of renormalizability and extended the RMF theory, with the systematic inclusion of new interactions by adding new terms to the model Lagrangian. This effective field theory motivated RMF (E-RMF) model calculations explained finite nuclei and nuclear matter with exactly same parameters and with significant accuracy in both the cases [26]. This approach can be considered as a salient step towards a unified and accurate theory for finite nuclei as well as for infinite nuclear matter. Extension of this model with the inclusion of the kaon (K^-) is the central interest of present work.

In NS, K^--condensation is one of the several possible transitions that could exist at high density. As the density of NS increases, the chemical potential of the negative electric charge (μ_e) also increases with the same rate of proton number density. Simultaneously, the effective mass of an in-medium K^- will decrease, due to the attractive interaction between K^- and nuclear matter. Therefore at a particular density (when μ_e is greater than energy of K^-), K^- replaces electron as neutralizing agent in charge-neutral matter. After the demonstration of interaction of K^- with the nuclear medium by Kaplan and Nelson [27], this topic acquired enormous interest. Glendenning and Schaffner-Bielich [17, 18], explained the interaction of K^- by coupling them to meson fields using a minimal coupling. This approach was followed by several other theoretical groups using RMF models [28–30]

*Electronic address: nehaguptaiitr@gmail.com

and has been adopted in this work as well.

In the present work we investigate the condensation from non-kaonic to kaonic phase, with different Lagrangians. In the presence of such a transition, we study the effect of higher order couplings on the EoS and hence on the NS properties. This work differs from many previous works in the sense that all the parameters used in E-RMF model were fitted to reproduce the observables of finite nuclei. Also, the E-RMF model is well tested throughout the nuclear chart by explaining several nuclear properties [31–36]. We show in this paper that this model explains the recent observations of NS as well.

In the section following this introduction, we describe the Lagrangian and field equations, both for non-kaonic and kaonic phases. This is followed by the expressions for energy density and pressure, which define the EoS. In section III we discuss the parameters used in our calculation. Our results and discussions are presented in section IV which is followed by the summary along with the conclusions drawn from present work.

II. EFFECTIVE FIELD THEORY MOTIVATED RELATIVISTIC MEAN FIELD MODEL WITH KAONS

In this section we briefly sketch the E-RMF model by presenting the model Lagrangian [25, 26]. We then show how the physical quantities, that will determine the composition of the NS, can be obtained self consistently.

The effective Lagrangian, obtained by curtailing terms irrelevant to nuclear matter in the E-RMF Lagrangian, can be written as

$$
\begin{aligned}
\mathcal{L} =\ & \bar{\psi}[g_\sigma \sigma - \gamma^\mu (g_\rho R_\mu + g_\omega V_\mu)]\psi \\
& + \frac{1}{2}\left(1 + \eta_1 \frac{g_\sigma \sigma}{m_n} + \frac{\eta_2}{2}\frac{g_\sigma^2 \sigma^2}{m_n^2}\right) m_\omega^2 V_\mu V^\mu \\
& + \frac{1}{4!}\zeta_0 g_\omega^2 (V_\mu V^\mu)^2 + \left(1 + \eta_\rho \frac{g_\sigma \sigma}{m_n}\right) m_\rho^2 \mathrm{tr}(R_\mu R^\mu) \\
& - m_\sigma^2 \sigma^2 \left(\frac{1}{2} + \frac{\kappa_3 g_\sigma \sigma}{3! m_n} + \frac{\kappa_4 g_\sigma^2 \sigma^2}{4! m_n^2}\right),
\end{aligned} \tag{1}
$$

where the scalar, vector and isovector meson fields and the nucleon field are denoted by σ, V_μ, R_μ and ψ respectively. m_σ, m_ω, and m_ρ are the corresponding meson masses and $m_n(= m_p)$ is the nucleon mass. The symbols g_σ, g_ω, g_ρ, κ_3, κ_4, η_1, η_2, η_ρ and ζ_0 denote the various coupling constants. More details of the Lagrangian are explained explicitly in Ref. [25].

Now we extend the E-RMF model by including a kaon (K^-)-nucleon interaction term. For simplicity, we choose that the kaon is coupled to the meson field with minimal coupling [17]. In this way, interactions of mesons with nucleons and kaons are treated in the same footing.

The Lagrangian for the kaon part reads

$$
\mathcal{L}_K = D_\mu^* K^* D^\mu K - m_K^{*2} K^* K, \tag{2}
$$

where the vector fields are coupled to kaons via the relation

$$
D_\mu = \partial_\mu + ig_{\omega K}V_\mu + ig_{\rho K}\tau_3 \cdot R_\mu, \tag{3}
$$

and m_K^* is the effective mass of kaon. The scalar field is coupled to kaons in a way analogous to the minimal coupling scheme [17] of the vector fields:

$$
m_K^* = m_K - g_{\sigma K}\sigma, \tag{4}
$$

where $m_K = 495$ MeV. Note that in the mean field approximation, only the time components of the vector fields V_0 contribute and charge conservation implies that only the third component in isospin-space of the isovector meson field R_0 does not vanish.

The dispersion relation for s-wave condensation ($\vec{k} = 0$), for K^- is

$$
\omega_K = m_K - g_{\sigma K}\sigma - g_{\omega K}V_0 - g_{\rho K}R_0, \tag{5}
$$

with K^- mesons having isospin projection $-1/2$. ω_K represents the K^- energy and is linear in the meson field. One can note that with the increase in density, ω_K decreases.

In the presence of K^-, equations of motion for the meson fields are

$$
\begin{aligned}
m_\sigma^2 \sigma =\ & g_\sigma \rho_s - \frac{m_\sigma^2 g_\sigma \sigma^2}{m_n}\left(\frac{\kappa_3}{2} + \kappa_4 \frac{g_\sigma \sigma}{3! m_n}\right) + \eta_\rho \frac{g_\sigma}{2m_n}m_\rho^2 R_0{}^2 \\
& + \frac{1}{2}\left(\eta_1 + \eta_2 \frac{g_\sigma \sigma}{m_n}\right)\frac{g_\sigma}{m_n}m_\omega^2 V_0^2 + g_{\sigma K}\rho_K,
\end{aligned}
$$

$$
\begin{aligned}
m_\omega^2 V_0 =\ & g_\omega (\rho_p + \rho_n) - \left(\eta_1 + \frac{\eta_2 g_\sigma \sigma}{2m_n}\right)\frac{g_\sigma \sigma}{m_n}m_\omega^2 V_0 \\
& - \frac{1}{3!}\zeta_0 g_\omega^2 V_0^3 - g_{\omega K}\rho_K,
\end{aligned}
$$

$$
m_\rho^2 R_0 = \frac{1}{2}g_\rho (\rho_p - \rho_n) - \eta_\rho \frac{g_\sigma \sigma}{m_n}m_\rho^2 R_0 - g_{\rho K}\rho_K, \tag{6}
$$

where ρ_s is the scalar density given by

$$
\rho_s = \frac{\gamma}{(2\pi)^3}\sum_{i=n,p}\int_0^{k_{fi}} d^3k \frac{m_n^*}{(k^2 + m_n^{*2})^{1/2}}, \tag{7}
$$

and γ is the spin-isospin degeneracy factor and is equal to 2 (for spin up and spin down). The nucleon effective mass is defined as in the standard Walecka model

$$
m_n^* = m_n - g_\sigma \sigma, \tag{8}
$$

and the K^- density is given by

$$
\rho_K = 2m_K^* K^* K = 2(\omega_K + g_{\omega K}V_0 + g_{\rho K}R_0)K^* K. \tag{9}
$$

The proton and neutron chemical potentials are

$$
\mu_p = \sqrt{k_{fp}^2 + m_n^{*2}} + g_\omega V_0 + \frac{1}{2}g_\rho R_0, \text{ and}
$$

$$
\mu_n = \sqrt{k_{fn}^2 + m_n^{*2}} + g_\omega V_0 - \frac{1}{2}g_\rho R_0. \tag{10}
$$

For a NS, in the absence of neutrino trapping, the conservation of baryon and electron chemical potentials leads to [37]

$$\mu_n = \mu_p + \mu_e,$$
$$\mu_e = \mu_\mu, \qquad (11)$$

and

$$q = \rho_p - \rho_e - \rho_\mu - \rho_K, \qquad (12)$$

where the first two constraints ensure the chemical equilibrium and the last one specifies the total charge which vanishes while imposing the charge neutrality. The total baryon density is

$$\rho = \rho_p + \rho_n \qquad (13)$$

The energy density can be written as

$$\epsilon = \epsilon_N + \epsilon_K, \qquad (14)$$

where ϵ_N is the energy density due to nucleons given by

$$
\begin{aligned}
\epsilon_N &= \sum_{i=n,p,l} \frac{\gamma}{(2\pi)^3} \int_0^{k_{fi}} d^3k \sqrt{k^2 + m_i^{*2}} - \frac{1}{4!}\zeta_0 g_\omega^2 V_0^4 \\
&- \frac{1}{2}\left(1 + \eta_1 \frac{g_\sigma \sigma}{m_n} + \frac{\eta_2}{2}\frac{g_\sigma^2 \sigma^2}{m_n^2}\right) m_\omega^2 V_0^2 + g_\omega V_0(\rho_p + \rho_n) \\
&- \frac{1}{2}\left(1 + \eta_\rho \frac{g_\sigma \sigma}{m_n}\right) m_\rho^2 R_0^2 + \frac{1}{2} g_\rho R_0(\rho_p - \rho_n) \\
&+ m_\sigma^2 \sigma^2 \left(\frac{1}{2} + \frac{\kappa_3}{3!}\frac{g_\sigma \sigma}{m_n} + \frac{\kappa_4}{4!}\frac{g_\sigma^2 \sigma^2}{m_n^2}\right),
\end{aligned} \qquad (15)
$$

and the energy density contributed by kaons is

$$\epsilon_K = 2m_K^{*2}K^*K = m_K^*\rho_K. \qquad (16)$$

Unlike the energy density, pressure is not directly affected by the inclusion of K^-, but the inclusion of K^- affects the fields and hence the pressure which reads

$$
\begin{aligned}
p &= \sum_{i=n,p,l} \frac{\gamma}{3(2\pi)^3} \int_0^{k_{fi}} d^3k \frac{k^2}{\sqrt{k^2 + m_i^{*2}}} + \frac{1}{4!}\zeta_0 g_\omega^2 V_0^4 \\
&+ \frac{1}{2}\left(1 + \eta_1 \frac{g_\sigma \sigma}{m_n} + \frac{\eta_2}{2}\frac{g_\sigma^2 \sigma^2}{m_n^2}\right) m_\omega^2 V_0^2 \\
&- m_\sigma^2 \sigma^2 \left(\frac{1}{2} + \frac{\kappa_3}{3!}\frac{g_\sigma \sigma}{m_n} + \frac{\kappa_4}{4!}\frac{g_\sigma^2 \sigma^2}{m_n^2}\right) \\
&+ \frac{1}{2}\left(1 + \eta_\rho \frac{g_\sigma \sigma}{m_n}\right) m_\rho^2 R_0^2.
\end{aligned} \qquad (17)
$$

Here l stands for the leptons (e^-, μ^-).

A. Non-kaonic phase (n, p, e^-, μ^-)

In the non-kaonic phase, vanishing charge density implies $q \equiv 0$ with $\rho_K = 0$. We can calculate σ, V_0, R_0, k_{fp}, k_{fn}, k_{fe}, and $k_{f\mu}$ by using Eqs. (6), (11), (12) and (13), at the chosen baryon density. When we get the converged solution for the above-listed quantities, the energy density and pressure can be computed from Eqs. (14) and (17).

B. Kaonic phase (n, p, e^-, μ^-, K^-)

With the solution of non-kaonic phase in hand, from Eq. (5) we can calculate kaon energy which keeps decreasing as we increase density, while μ_e increases. When the condition $\omega_K = \mu_e$ is first achieved, the kaon will occupy a small fraction of the total volume and the charge density corresponding to kaonic phase, $q \equiv 0$. We can calculate σ, V_0, R_0, k_{fp}, k_{fn}, k_{fe}, $k_{f\mu}$ and ρ_K by using Eqs. (6), (11) (12) and (13) with the condition $\omega_K = \mu_e$, for any chosen baryon density. After getting these solutions, we can calculate energy density and pressure for kaonic phase, using Eqs. (14) and (17).

III. CHOICE OF PARAMETERS

In the present work we have chosen five sets of parameters namely NL1 [38], NL3 [39], G1, G2 [32] and FSUGold [22]. The first two parameter sets correspond to the standard RMF model with very different compressibilities $[K_\infty(\text{NL1}) = 212$ MeV and $K_\infty(\text{NL3}) = 271.76$ MeV]. In the case of FSUGold, there are two more coupling parameters Λ and ζ_0 in comparison to NL1 and NL3 parameter sets. These parameters represent the strength of the self-interaction of vector field (ζ_0) and the isoscalar -isovector mixing (Λ). The interactions G1 and G2 correspond to the complete E-RMF Lagrangian discussed in the earlier section. One can note that in comparison to NL1 and NL3, G1 and G2 have four more coupling constants ($\eta_1, \eta_2, \eta_\rho$, and ζ_0). All the coupling constants are obtained by fit to several properties of finite nuclei [25]. It is worth to mention that in this case no parameter is treated as adjustable and the fitting does not involve any observation at densities above the saturation value. Since the expectation value of the R_0 field is typically an order of magnitude smaller than that of the V_0 field, in the E-RMF model, the nonlinear R_0 couplings were retained only through third order [25]. However, it has been shown that the isoscalar-isovector mixing $(\Lambda(g_\omega V_0)^2(g_\rho R_0)^2)$ is useful to modify the neutron radius in heavy nuclei while making very small changes to the proton radius and the binding energy [21, 22].

In the effective Lagrangian approach adopted here, knowledge of two distinct sets of coupling constants — one parametrizing the nucleon-nucleon interaction and one parametrizing the kaon-nucleon interactions — is required for numerical computations. We discuss each of these in turn.

A. Nucleon coupling constants

The symbols g_σ, g_ω, g_ρ, κ_3, κ_4, η_1, η_2, η_ρ, ζ_0 and Λ denote the nucleon coupling constants. At times these constants bear different values in literature for the same parameter set. For example, for the set NL1 different numbers are quoted in Refs. [38] and [39] but they yield

TABLE I: Parameters and the saturation properties for NL1[38], NL3[39], G1, G2[32], and FSUGold[22]. The parameters g_σ, g_ω, g_ρ, κ_3 and κ_4 are calculated from the given saturation properties using relations suggested in Ref. [37] with the exception of FSUGold where all the coupling constants are taken from Ref. [22].

	NL1	NL3	G1	G2	FSUGold
m_n (MeV)	938	939	939	939	939
m_σ (MeV)	492.25	508.194	507.06	520.206	491.5
m_ω (MeV)	795.36	782.501	782	782	783
m_ρ (MeV)	763	763	770	770	763
g_σ	10.0730	10.1756	9.8749	10.5088	10.5924
g_ω	13.1917	12.7885	12.1270	12.7864	14.3020
g_ρ	9.8553	8.9849	8.7886	9.5108	11.7673
κ_3	1.8324	1.4841	2.2075	3.2376	0.6194
κ_4	-7.7099	-5.6596	-10.0808	0.6939	9.7466
η_1	0	0	0.071	0.65	0
η_2	0	0	-0.962	0.11	0
η_ρ	0	0	-0.272	0.390	0
ζ_0	0	0	3.5249	2.642	0.06
Λ	0	0	0	0	0.03
ρ_0 (fm^{-3})	0.154	0.148	0.153	0.153	0.148
(E/A)(MeV)	-16.43	-16.299	-16.14	-16.07	-16.3
K_∞(MeV)	212	271.76	215	215	230
J(MeV)	43.6	37.4	38.5	36.4	32.59
m_n^*/m_n	0.571	0.6	0.634	0.664	0.609^a

$^a m_n^*$ for FSUGold was calculated from the coupling constants.

same saturation properties. Among the above-mentioned coupling constants, g_σ, g_ω, g_ρ, κ_3 and κ_4 can be written algebraically in terms of empirical quantities: ρ_0, E/A, K_∞, J, m_n^* and vice versa [37]. Using these relations we have calculated g_σ, g_ω, g_ρ, κ_3 and κ_4 in the case of NL1 [38], NL3 [39], G1 and G2 [32]. These calculated parameters, and other parameters taken from corresponding references are listed in Table I. In case of FSUGold, all the coupling constants are taken from Ref. [22].

B. Kaon coupling constants

In order to investigate the effect of kaons on the high density matter, the kaon-nucleon coupling constant has to be specified. The laboratory experiments give information only about kaon-nucleon interaction in free space. In this work we mainly focus on the NS (densities $\gg \rho_0$), and therefore the kaon-nucleon interaction determined from experiment need not be appropriate for our calculations. The interaction of omega and rho mesons with kaon ($g_{\omega K}$ and $g_{\rho K}$) can be determined using a simple quark and isospin counting argument [17] given by,

$$g_{\omega K} = \frac{1}{3}g_\omega \text{ and } g_{\rho K} = \frac{1}{2}g_\rho \ . \tag{18}$$

We can specify the interaction of sigma meson with kaon ($g_{\sigma K}$) using its relation with the optical potential of a single kaon in infinite matter (U_K):

$$U_K = -g_{\sigma K}\sigma(\rho_0) - g_{\omega K}V_0(\rho_0), \tag{19}$$

where typically we have $-80 \text{ MeV} \lesssim U_K \lesssim -180 \text{ MeV}$ [40, 41].

IV. RESULTS AND DISCUSSIONS

The quality of different interactions in explaining symmetric matter and pure neutron matter properties at higher densities than the normal nuclear densities has been discussed in Refs. [26, 42], by comparing the calculated pressure with the experimental data [43]. This comparison clearly suggests a softer EoS for symmetric matter, which could be obtained only with higher order couplings in the Lagrangian. The pure neutron matter data, though model dependent, also was found to favour a softer EoS. One important observation highlighted in Ref. [26], is that the softness in EoS from G1, G2 and FSUGold is mainly due to the new couplings and not due to the difference in compressibility as usually perceived. For example, the compressibility from NL1 (K_∞=212) and G1, G2 (K_∞=215) are very similar but the EoS at higher densities are completely different. NL1 (K_∞=212) and NL3 (K_∞=271.76) yield different compressibilities but their EoS are more similar. The role of higher order couplings in softening the EoS has been discussed in Ref. [42] for the case of FSUGold. EoS from FSUGold is softer than that of G2 because of the large and positive κ_4 value as well as the introduction of isoscalar-isovector coupling (Λ). In fact it has been clearly demonstrated [21, 44] that Λ softens the symmetry energy considerably.
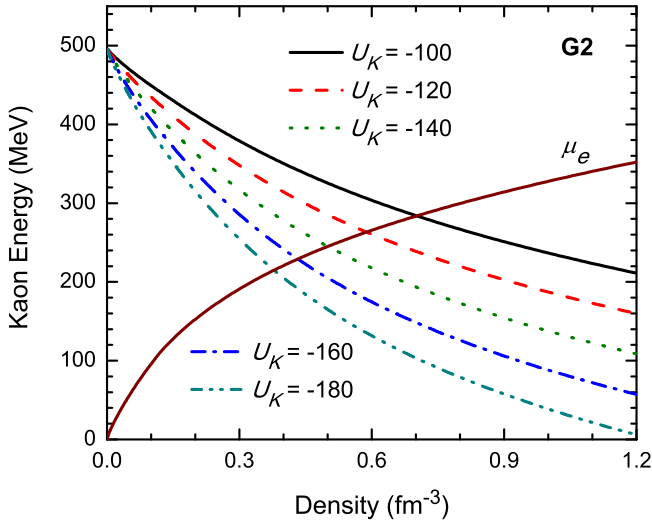
FIG. 1: (Color online) The density dependence of the K^- energy (ω_K) in NS matter for different optical potentials (U_K in MeV) calculated with G2 parameter set. The point at which electron chemical potential (μ_e) intersects ω_K defines the onset of K^--condensation.
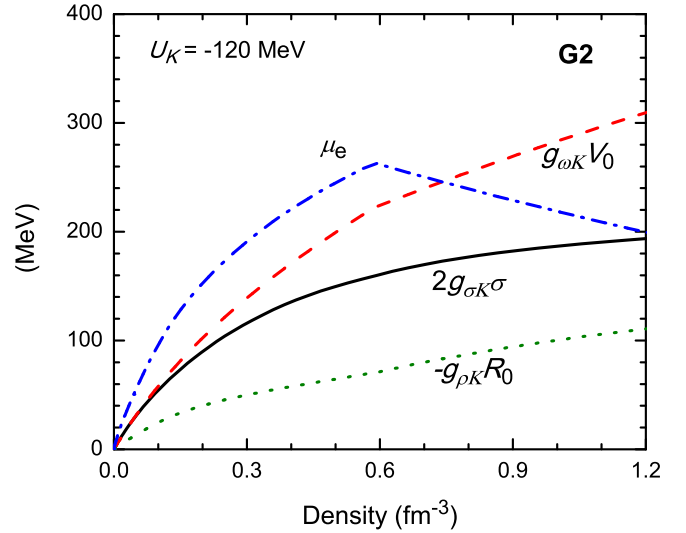

FIG. 2: (Color online) The density dependence of the scalar ($g_{\sigma K}\sigma$), vector ($g_{\omega K}V_0$), and iso-vector ($g_{\rho K}R_0$) fields in the NS matter inclusive of kaonic phase, calculated with G2 parameter set.

The success of G1 and G2 in explaining the high density EoS constrained by phenomenological flow analysis [43], has been carried forward in explaining NS properties as well [26]. FSUGold also has been successful in explaining both these features [22, 42]. Henceforth we discuss the role of new parameters of extended RMF models on the onset and effect of kaon condensation in NS. Among the different parameter sets considered here (Table I) G2 and FSUGold have a positive quartic scalar self-coupling (κ_4), which is more meaningful than a negative one [26, 45]. For this reason we prefer the set G2, when we have to choose between G1 and G2.

A. Results from G2

In Fig. 1, we have presented the K^- energy (ω_K) for different optical potentials, as a function of density along with the variation of electron chemical potential (μ_e). The ω_K decreases with increasing density [Eq. (5)] while μ_e increases. When ω_K is lower than μ_e, K^- are favoured (due to attraction between K^- and nucleon) to replace electrons while contributing to the charge neutrality. From Fig. 1, it is evident that the onset of K^--condensation is strongly modified by the strength of the kaon optical potential (U_K). Calculations based on chiral models [41] suggest that a value $U_K = -120$ MeV is more appropriate for NS. Hence in most of the further discussions we choose $U_K = -120$ MeV and look at the other dependencies for the EoS of NS.

The σ, ω, and ρ fields calculated for NS at $U_K = -120$ MeV are presented in Fig. 2 along with the μ_e. The density at which K^- starts to contribute can be read from the point where the μ_e shows a sharp kink (~ 0.6
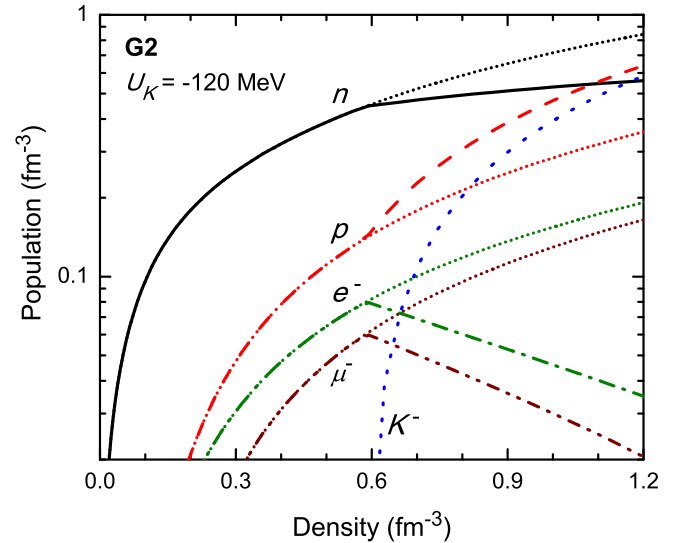

FIG. 3: (Color online) The relative population of hadrons and leptons in NS as a function of baryon density calculated with G2 parameter set. The calculations done without considering kaons are represented by the small-dotted lines.

fm^{-3}). Though the corresponding kinks in the fields are very subtle, any small change in the field results in a significant change in energy density and pressure. The presence of K^- alters the proton-neutron ratio and hence the contribution from the ρ field is enhanced. This is due to the fact that the processes like $n \rightarrow p + K^-$ are more energetically favoured than processes like $n \rightarrow p + e^-$ at higher densities where K^- energy is decreasing and μ_e is increasing [See Fig. 1]. From Fig. 2 we can also see that the K^- has very less influence on the σ field. In other words, for the parameters considered here, the
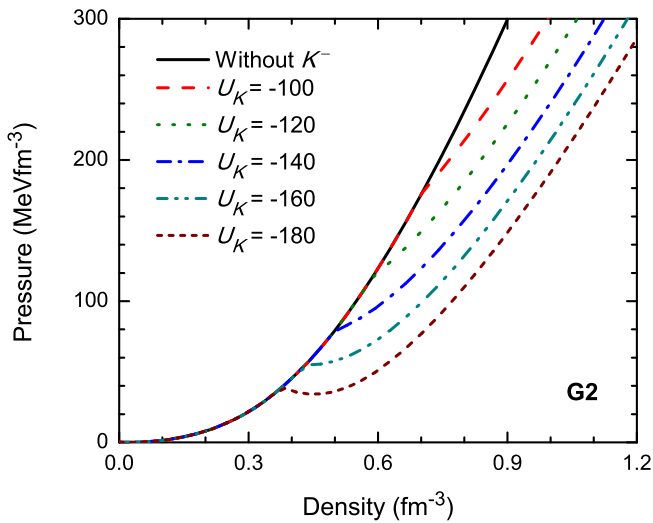
FIG. 4: (Color online) Pressure in NS matter versus baryon density calculated using different optical potentials and G2 parameter set.
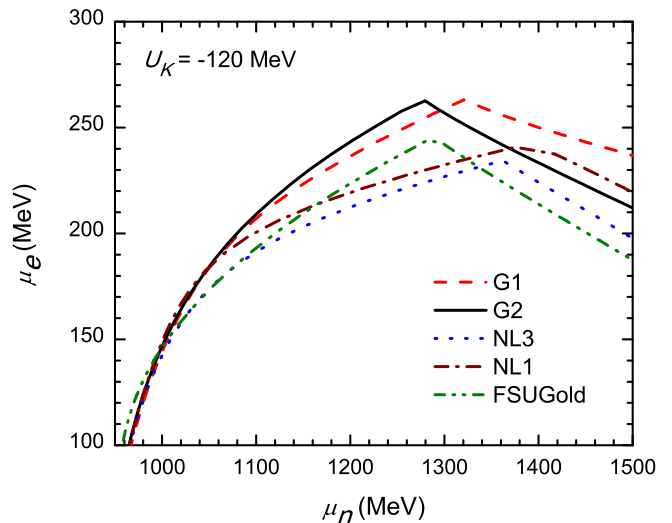

FIG. 5: (Color online) The electron chemical potential versus the neutron chemical potential in NS matter calculated with different parameter sets. The kinks represent transition from non-kaonic to kaonic phase.

attraction caused by K^- is weak in comparison with that of σ mesons.

The appearance of K^- at higher densities and its role in population (number density) of different particles are presented in Fig. 3. As soon as K^--condensation sets in, the population of K^- rapidly increases with density and hence allows the presence of more protons. Interestingly, at very high densities the number of protons exceed that of the neutrons, which is not the case if K^- were not present. This can be seen from the corresponding deviation from the non-kaonic matter trends. Apart from the arguments given earlier, the reason for p-K^- pairs being preferred to neutrons is quantitatively very well explained by Glendenning and Schaffner-Bielich [17]. However, the symmetry term in the energy obviously prefer a symmetric matter and hence hinders the protons to be populated much more than neutrons. All the above-mentioned effects have a significant role to play in determining the EoS which is discussed in the following text.

Our results for the pressure calculated with G2 parameter set and with different optical potentials for K^- are presented in Fig. 4. On first sight one can appreciate the strong influence of U_K in softening the EoS, which is similar to the results of many previous works. Also for lower values of U_K, the graph suggests a second order phase transition from a non-kaonic to kaonic phase. Only with a very high value of $U_K (\gtrsim -160 \text{ MeV})$ one can have a first order phase transition. This is rather consistent with the observation in Ref. [29] where higher order interactions are included using the lowest order chiral Lagrangian. However, the role of more general higher order operators was considered to be an open question which is answered in the present work. One may expect some changes in the onset of K^--condensation if we consider the presence of a mixed phase (of kaonic and non-kaonic phases) [17]. The presence of such a mixed phase is nor-

mally possible in first order K^--condensation where one gets a dip in the pressure like the one for $U_K \gtrsim -160$ MeV as shown in Fig. 4. This argument implies that the presence of mixed phase is not favoured in our case for $U_K < -160$ MeV. The main observation from Fig. 4 is that even in the presence of higher order couplings, the presence of K^- dramatically softens the EoS and the softness is proportional to U_K.

B. Comparison between different interactions

So far we have discussed our results with the G2 parameter set and in this section we analyze how our results compare with different interactions considered in this work. In Fig. 5 we show the chemical potentials which indicate the onset of K^--condensation for different parameters. The maximum value of μ_e (μ_e^{max}) denotes the point at which the transition happens and is seen to be larger for G1 and G2. μ_e^{max} is almost same for NL1 and FSUGold and the least value is for NL3. μ_e^{max} also quantifies the number density of electrons which falls sharply when K^- starts to appear [See Fig. 3]. Both μ_e^{max} and the μ_n values at which the transition happens (μ_n^c), strongly depend on the interaction. μ_n^c for G2 and FSUGold are more closer resulting from a closer EoS. A sharper kink in Fig. 5, leading to a situation where there could be more than one value of μ_e for a given μ_n, would have indicated a first order phase transition. It is clear that for $U_K = -120$ MeV, all the interactions lead only to a second order phase transition where a mixed phase cannot appear.

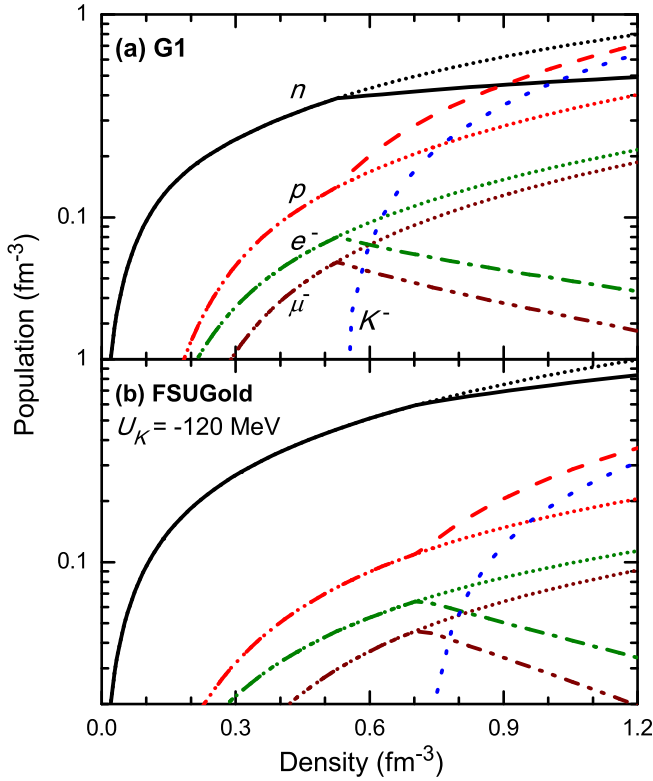In Fig. 6 we compare the number densities arising from the calculations with G1 and FSUGold, which can be

FIG. 6: (Color online) The relative population of hadrons and leptons in NS matter as function of baryon density calculated with (a) G1 and (b) FSUGold parameter sets. The calculations done without considering kaons are represented by the small-dotted lines.

FIG. 7: (Color online) Density dependence of the electron chemical potential (μ_e) and K^- energy (ω_K) for different parameters. The point at which μ_e intersects ω_K defines the onset of K^--condensation.

FIG. 8: (Color online) The EoS for non-kaonic and kaonic NS matter obtained from various parameter sets. The calculations done without considering kaons are represented by the small-dotted lines whereas the calculations with kaons are represented by different line patterns as given in the legends. The solid circles correspond to the values at the center of maximum mass NS. Solid squares represent the observational extraction [46], however not uniquely constrained [42].

compared with Fig. 3 as well. The results for G1 are very similar to that of G2 except for the early onset of K^--condensation in G1. Between Figs. 6 (a) and (b), we can see a significant difference in the relative population between protons and neutrons at higher densities. This is mainly due to the interplay between ω_K and μ_e which are plotted in Fig. 7. The decrease in ω_K or increase in μ_e favours more of K^- and hence protons. ω_K varies linearly with the meson fields as given in Eq. (5) and should reflect the stiffness of the fields and hence that of the EoS. We can see in Fig. 7 that the ω_K for NL3 is quite different from others due to the fact that the EoS of NL3 is quite stiffer than others [26, 42]. This stiffness arises from the vector potential which grows almost as a straight line [32]. The quartic vector self-interaction brings down the vector potential and makes the equation of state and hence ω_K softer in other cases. The other quantity determining the onset of K^--condensation is $\mu_e(= \mu_n - \mu_p)$ which has terms similar to that of the symmetry energy and is dominated by the R_0 field [Eq. (10)]. Thus the density dependence of symmetry energy directly affects μ_e and is crucial in determining the onset of K^--condensation. NL3, G1 and G2 yield similar symmetry energy (not shown here) and the unique isoscalar-isovector mixing $(\Lambda(g_\omega V_0)^2(g_\rho R_0)^2)$ in FSUG-
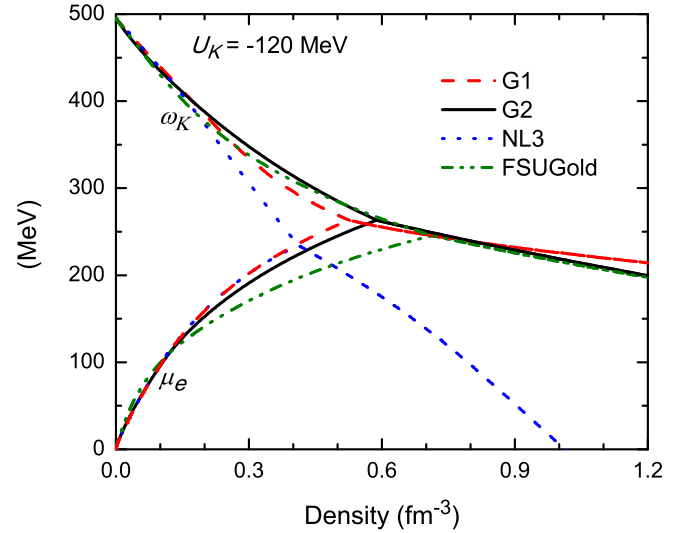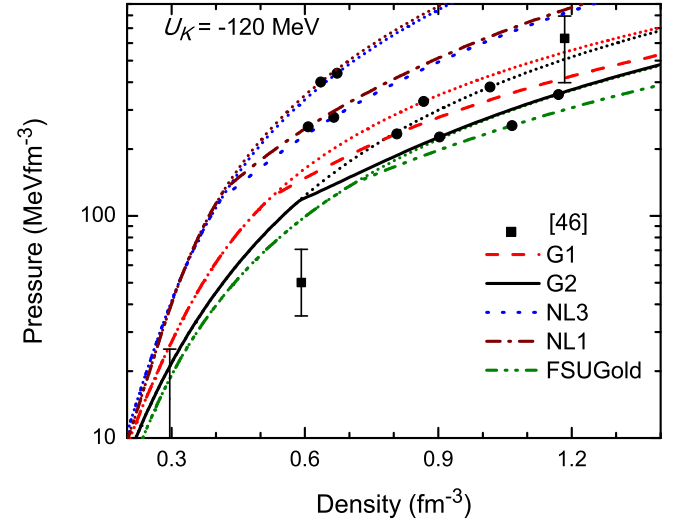
old suppresses the R_0 field which leads to a softer symmetry energy and hence lesser μ_e.

If we compare between G2 and FSUGold, μ_e(G2) $> \mu_e$(FSUGold) and with similar ω_K, kaons are more favoured for larger μ_e. Lesser kaons in FSUGold leads to lesser number of protons at higher densities in Fig. 6 (b). In Fig. 7 one can see that the μ_e for NL3 and G1 are almost same till the transition point. However due to
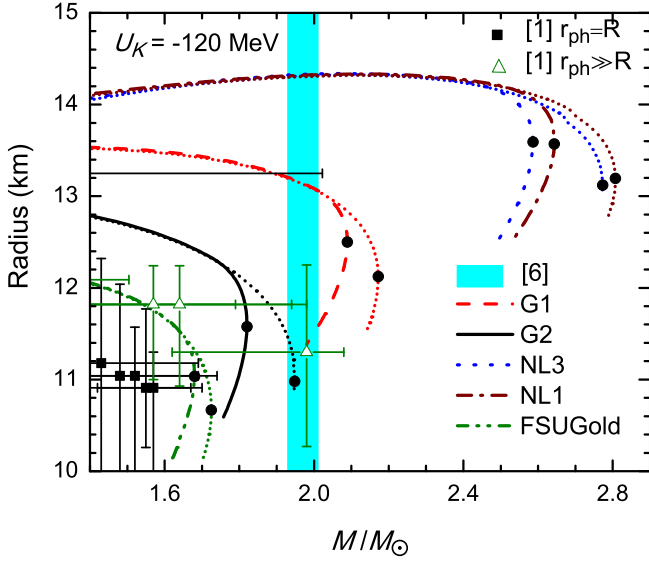
FIG. 9: (Color online) The mass-radius relation for non-kaonic and kaonic phases using different parameter sets. The calculations done without considering kaons are represented by the small-dotted lines. The solid circles represent the maximum mass in every case. Mass is given in units of solar mass $M_\odot$. Solid squares ($r_{ph} = R$) and open triangles ($r_{ph} \gg R$) represent the observational constraints [1], where r_{ph} is the photospheric radius. The shaded region correspond to the recent observation of $1.97 \pm 0.04 M_\odot$ star [6].
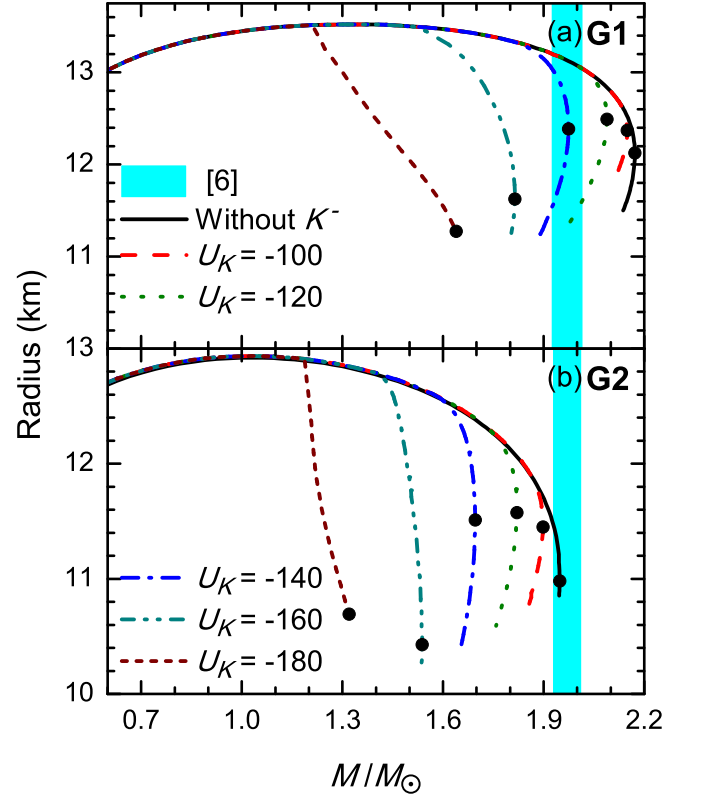

FIG. 10: (Color online) The mass-radius relation for NS calculated using different optical potentials and with G2 parameter set. Mass is in units of solar mass $M_\odot$ and U_K are in MeV. The solid circles represent the maximum mass in every case.

the large difference in ω_K, which falls very sharply in the case of NL3, K^--condensation occurs at a smaller density in NL3 when compared with G1. These features can be seen from the EoS presented in Fig. 8 as well.

Figure 8 shows the pressure calculated with the different interactions, with and without the inclusion of K^-. Similar to the case of symmetric and pure neutron matter [26, 42], the higher order couplings in G1, G2 and FSUGold lead to a softer EoS. All the interactions suggest a major change in pressure when we include K^-. The well known feature of K^- making the EoS softer, can also be seen clearly in Fig. 8. For both kaonic and non-kaonic phases, the difference between pressure obtained from G1 and G2 changes with density. Around $\rho \sim 0.5$ fm^{-3}, the difference is maximum and it decreases as the density increase. This is due to the interplay between the terms with higher order couplings ($\kappa_3, \kappa_4, \eta_2$) which can give negative contribution to pressure. Between G1 and G2, the sign of the coupling constants κ_4, η_2, and η_ρ differ. Among these three couplings, the term comprising η_ρ is weaker. In the case of G1, due to the change in sign of κ_4, the combined effect of κ_3 and κ_4 on pressure is negligible. Hence in G1, η_2 dominates at higher densities in reducing the pressure. In case of G2, the contribution from terms having κ_4 and η_2 is negligible and κ_3 dominates at higher densities in reducing the pressure. Thus in G1 and G2, η_2 (quartic scalar-vector cross-interaction), and κ_3 (cubic scalar self-interaction) respectively, rule the suppression of pressure at very high densities. η_2 being associated

with the vector self-interaction is much stronger at high densities and hence will be more effective than κ_3 in reducing the pressure. Couplings defined by η_2 and κ_3 are of different order and will naturally yield results of different curvature which leads to the varying difference in pressure between G1 and G2. The difference in pressure from G2 and FSUGold is well reduced in the presence of K^-, even at higher energies. Interestingly, G2 with K^- yields same pressure as that of FSUGold without K^- and in a broad energy range these results cease to differ. However, the corresponding energy densities are very different (not shown here) and hence the resulting maximum mass NS have different central densities (represented by solid circles in Fig. 8). The EoS around the region of central density is more dominant in determining the properties of NS. This region is quite different for different parameters. Also one can see that the central density increases with softer EoS, and the presence of K^- decreases the central density and pressure.

The change in central density ($\Delta\rho_c$) due to K^- depends mostly on the following three quantities, viz.,

(i) density at which K^--condensation sets in (ρ_B^K) with $\Delta\rho_c \propto 1/\rho_B^K$,

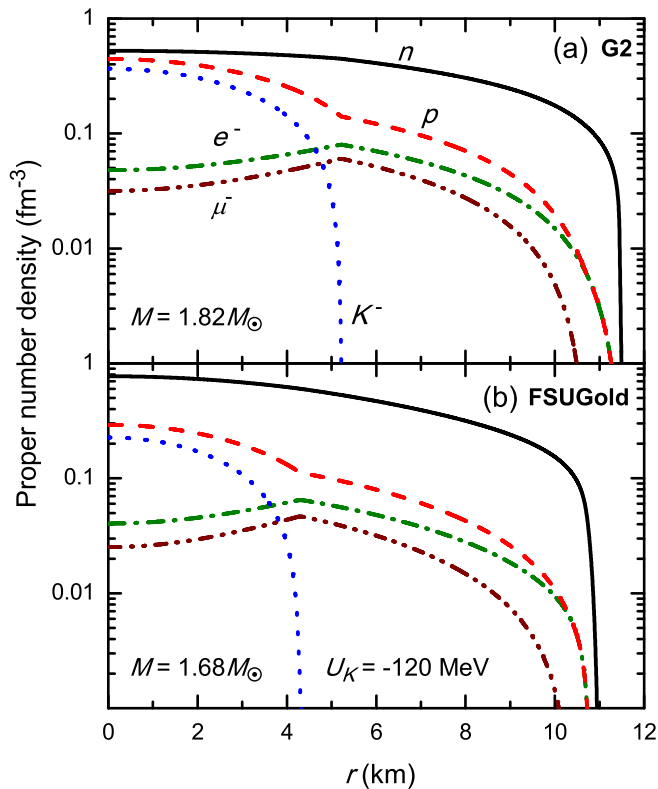(ii) the magnitude of central density with $\Delta\rho_c \propto \rho_c$, and

FIG. 11: (Color online) The composition of maximum mass NS as a function of radial distance calculated using FSUGold and G2 parameter sets.

(iii) the stiffness of EoS at ρ_c, with stiffer EoS leading to larger $\Delta\rho_c$.

The interplay of the above quantities gives arise to varying $\Delta\rho_c$ for different parameters. For example, between G1 and G2, quantities (ii) and (iii) dominate (i), resulting in a larger $\Delta\rho_c$ in case of G2. These effects should naturally be seen in the calculation of maximum mass and radius of NS.

We can obtain mass-radius relation for NS by solving the well-known Tolman–Oppenheimer–Volkoff (TOV) equations [47, 48]. The results for mass-radius relation in NS are given in Fig. 9 where the calculations are done using different interactions, without and with the K^- ($U_K = -120$ MeV). The RMF models NL3 and NL1 suggest very large and massive NS. In these cases though the maximum mass is reduced considerably (from ~ 2.8 $M_\odot$ to ~ 2.4 $M_\odot$) in the presence of kaons, these are overshooting the observational constraints for NS [1–6]. Though G1 and G2 are from the same E-RMF model with same terms in the Lagrangian, their results for NS are quite different with G1 suggesting a larger and heavier NS. As explained earlier, G1 and G2 yield EoS of different nature and have varying role of K^-. The result for G2 and FSUGold are the closest ones. Very interestingly, though their difference is larger when K^- are not considered, the presence of K^- brings these two results

closer. This is the direct implication of the same feature we observed in the case pressure (Fig. 8). The G2 interaction allows more K^- to be present (due to early onset of K^--condensation) and hence makes the EoS more softer which eventually get closer to that of FSUGold. The observed reduction of maximum mass due to kaons, in case of NL3 and FSUGold is consistent with the values quoted in Ref. [23]. Overall, in the presence of K^-, the mass decreases and the radius corresponding to maximum mass increases. All the observational constraints shown in Fig. 9 favor the models with higher order couplings but most of these constrains cover a broad range which may not be precise enough to ascertain the presence of kaons.

In Fig. 10, we show the dependence of NS mass-radius on U_K with G2 parameter set. We can see clearly that the stronger U_K increases the contribution of K^- which results in softer EoS which in turn yields a smaller and lighter NS. The typical hook shape of the mass-radius curve is maintained till $U_K \lesssim -160$ MeV and beyond that the curve takes a straight dip which is a characteristic of first order K^--condensation. It is interesting to note that without K^-, the maximum mass given by G2 ($1.95M_\odot$) is closer to the one suggested by Demorest et al. ($1.97 \pm 0.04 M_\odot$) [6] with a radius of 11.03 km. G1 with $U_K = -140$ MeV (graph not shown here) suggests a maximum mass of $1.97M_\odot$ with a radius of 12.45 km.

Figure 11 shows the number density versus the radial distance from the center of NS, calculated with G2 and FSUGold parameter sets, when the NS is having the maximum mass ($1.68M_\odot$ for FSUGold, and $1.82M_\odot$ for G2 with $U_K = -120$ MeV). The behaviour of number densities shown in Fig. 11 is directly reflecting the patterns shown for relative populations plotted against density in Figs. 3 and 6 (b). The difference between the radii of kaonic matter suggested by G2 and FSUGold is almost one km. Another striking difference in the composition of NS is the asymmetry of the core. G2 suggests a nearly symmetric matter at the core whereas FSUGold indicates highly neutron-rich core. We have seen that this trend remains same even at higher values of U_K (not shown here). It will be interesting to see how the presence of hyperons affect the overall scenario [49].

V. SUMMARY

In the present work, we have studied the role of higher order couplings of extended RMF models on the onset and effect of kaon (K^-) condensation in neutron stars (NS). We have calculated the NS properties with the successful RMF parameters NL1 and NL3, the E-RMF parameters G1 and G2 (four additional couplings to RMF), and the FSUGold parameters (two additional couplings to RMF).

In extended RMF models, with most common values of kaon optical potential ($U_K \lesssim -160$ MeV), the transition from a non-kaonic phase to kaonic phase in NS has a

character of second order which rules out the possibility of having a mixed phase of kaonic and non-kaonic matter. This is consistent with the observation in Ref. [29] where higher order interactions are included using the lowest order chiral Lagrangian. The role of more general higher order operators was considered to be an open question and we have shown that they lead to a second order phase transition. This justifies the neglect of mixed phase in our calculations mostly done with $U_K = -120$ MeV [41].

Apart from the usual dependence on U_K reported elsewhere [17, 29], the onset of kaon condensation in NS strongly depends on the parameters of Lagrangian especially the higher order couplings. This is due to the strong variation in density dependence of the K^- energy (ω_K) and electron chemical potential (μ_e) whose interplay determine the onset of K^--condensation. Density dependence of ω_K is similar to that of EoS and μ_e varies in a way similar to symmetry energy. So, any change in the density dependence of EoS or that of symmetry energy will affect the onset as well as the effect of K^--condensation. Without higher order couplings, NL1 and NL3 have stiffer EoS than others which leads to a stiffer ω_K and hence a early onset of K^--condensation. FSUGold comprises an unique isoscalar-isovector mixing which leads to a softer symmetry energy and hence a delayed onset of K^--condensation.

The central density of NS increases with softer EoS, and the presence of K^- decreases the central density and pressure. The change in central density due to the presence of K^- is different for different parameters due to the interplay between (i) the density defining onset of K^--condensation, (ii) the central density (ρ_c) itself, and (iii) the stiffness of EoS at ρ_c. Due to this, the impact of K^- is more pronounced in G2 than in G1 and is weakest in FSUGold. All these effects are strongly reflected in the calculation of mass-radius relation of NS. The NS suggested by models without higher order couplings (NL3 and NL1) contradict the observational constraints [1–6] even with the inclusion of K^-. The higher order couplings play a dominant role (than kaons) in bringing the mass and radius of NS within observed limits. Different parameter sets lead to different concentration of kaons (which is known to affect the population of protons [17]) in NS, and hence lead to different asymmetries in the core of NS. We have shown that G1 and G2 suggest a symmetric core whereas FSUGold suggests a neutron rich core due to lesser amount of K^- caused by an unique coupling which softens the symmetry energy.

We conclude that the extended RMF models, which are quite successful in explaining several properties of finite nuclei, suggest a strong influence of higher order couplings and kaons in NS whose properties are within the present observational constraints [1–6].

[1] A. W. Steiner, J. M. Lattimer, and E. F. Brown, Astrophys. J **722**, 33 (2010).
[2] D. J. Champion et al., Science **320**, 1309 (2008).
[3] S. M. Ransom et al., Science **307**, 892 (2005).
[4] P. C. C. Freire, A. Wolszczan, M. van den Berg, and J. W. T. Hessels, Astrophys. J. **679**, 1433 (2008).
[5] A. van der Meer, L. Kaper, M. H. van Kerkwijk, M. H. M. Heemskerk, and E. P. J. van den Heuvel, Astron. Astrophys. **473**, 523 (2007).
[6] P. B. Demorest, T. Pennucci, S. M. Ransom, M. S. E. Roberts, and J. W. T. Hessels, Nature **467**, 1081 (2010).
[7] J. M. Lattimer and M. Prakash, Astrophys. J. **550**, 426 (2001).
[8] B. Friedman and V. R. Pandharipande, Nucl. Phys. A **361**, 502 (1981).
[9] R. B. Wiringa, V. Fiks, and A. Fabrocini, Phys. Rev. C **38**, 1010 (1988).
[10] A. Akmal and V. R. Pandharipande, Phys. Rev. C **56**, 2261 (1997).
[11] H. Müller and B. D. Serot, Nucl. Phys. A **606**, 508 (1996).
[12] H. Müther, M. Prakash, and T. L. Ainsworth, Phys. Lett. B **199**, 469 (1987).
[13] L. Engvik, E. Osnes, M. Hjorth-Jensen, G. Bao, and E. Ostgaard, Astrophys. J. **469**, 794 (1996).
[14] N. K. Glendenning and S. A. Moszkowski, Phys. Rev. Lett. **67**, 2414 (1991).
[15] V. R. Pandharipande and R. A. Smith, Nucl. Phys. A **237**, 507 (1975).
[16] M. Prakash, J. R. Cooke, and J. M. Lattimer, Phys. Rev. D **52**, 661 (1995).
[17] N. K. Glendenning and J. Schaffner-Bielich, Phys. Rev. C **60**, 025803 (1999).
[18] N. K. Glendenning and J. Schaffner-Bielich, Phys. Rev. Lett. **81**, 4564 (1998).
[19] M. Uchida, H. Sakaguchi, M. Itoh, M. Yosoi, T. Kawabata, H. Takeda, Y. Yasuda, T. Murakami, T. Ishikawa, T. Taki, et al., Phys. Lett. B **557**, 12 (2003).
[20] T. Li, U. Garg, Y. Liu, R. Marks, B. K. Nayak, P. V. M. Rao, M. Fujiwara, H. Hashimoto, K. Kawase, K. Nakanishi, et al., Phys. Rev. Lett. **99**, 162503 (2007).
[21] C. J. Horowitz and J. Piekarewicz, Phys. Rev. C **64**, 062802 (2001).
[22] B. G. Todd-Rutel and J. Piekarewicz, Phys. Rev. Lett. **95**, 122501 (2005).
[23] B. K. Sharma and S. Pal, Phys. Lett. B. **682**, 23 (2009).
[24] Y. K. Gambhir, P. Ring, and A. Thimet, Ann. Phys. (N.Y.) **198**, 132 (1990).
[25] R. J. Furnstahl, B. D. Serot, and H.-B. Tang, Nucl. Phys. A **615**, 441 (1997).
[26] P. Arumugam, B. K. Sharma, P. K. Sahu, S. K. Patra, T. Sil, M. Centelles, and X. Viñas, Phys. Lett. B **601**, 51 (2004).
[27] D. B. Kaplan and A. E. Nelson, Phys. Lett. B **175**, 57 (1986).
[28] T. Norsen and S. Reddy, Phys. Rev. C **63**, 065804 (2001).
[29] J. A. Pons, S. Reddy, P. J. Ellis, M. Prakash, and J. M. Lattimer, Phys. Rev. C **62**, 035803 (2000).
[30] G.-h. Wang, W.-j. Fu, and Y.-x. Liu, Phys. Rev. C **76**, 065802 (2007).
[31] M. D. Estal, M. Centelles, and X. Viñas, Nucl. Phys. A

650, 443 (1999).

[32] M. D. Estal, M. Centelles, X. Viñas, and S. K. Patra, Phys. Rev. C **63**, 024314 (2001).

[33] M. D. Estal, M. Centelles, X. Viñas, and S. K. Patra, Phys. Rev. C **63**, 044321 (2001).

[34] T. Sil, S. K. Patra, B. K. Sharma, M. Centelles, and X. Viñas, Phys. Rev. C **69**, 044315 (2004).

[35] X. Roca-Maza, M. Centelles, F. Salvat, and X. Viñas, Phys. Rev. C **78**, 044332 (2008).

[36] A. Shukla, B. K. Sharma, R. Chandra, P. Arumugam, and S. K. Patra, Phys. Rev. C **76**, 034601 (2007).

[37] N. K. Glendenning, *Compact Stars* (Springer-Verlag, New York, 2007), 2nd ed.

[38] P. G. Reinhard, M. Rufa, J. Maruhn, W. Greiner, and J. Friedrich, Z. Phys. A **323**, 13 (1986).

[39] G. A. Lalazissis, J. König, and P. Ring, Phys. Rev. C **55**, 540 (1997).

[40] V. Koch, Phys. Lett. B **337**, 7 (1994).

[41] T. Waas and W. Weise, Nucl. Phys. A **625**, 287 (1997).

[42] F. J. Fattoyev, C. J. Horowitz, J. Piekarewicz, and G. Shen, Phys. Rev. C **82**, 055803 (2010).

[43] P. Danielewicz, R. Lacey, and W. G. Lynch, Science **298**, 1592 (2002).

[44] C. J. Horowitz and J. Piekarewicz, Phys. Rev. Lett. **86**, 5647 (2001).

[45] V. G. Gueorguiev, W. E. Ormand, C. W. Johnson, and J. P. Draayer, Phys. Rev. C **65**, 024314 (2002).

[46] F. Özel, G. Baym, and T. Güver, Phys. Rev. D **82**, 101301 (2010).

[47] J. R. Oppenheimer and G. M. Volkoff, Phys. Rev. **55**, 374 (1939).

[48] R. C. Tolman, Phys. Rev. **55**, 364 (1939).

[49] S. Banik and D. Bandyopadhyay, Phys. Rev. C. **64**, 055805 (2001).